Journal of Chromatography B 1210 (2022) 123449

Contents lists available at ScienceDirect

Journal of Chromatography B

journal homepage: www.elsevier.com/locate/jchromb

Factors affecting robustness of anion exchange chromatography: Selective retention of minute virus of mice using membrane media

Shu-Ting Chen [a], Wenbo Xu [b], Kang Cai [c], Gisela Ferreira [c], S. Ranil Wickramasinghe [a], Xianghong Qian [b,*]

[a] Department of Chemical Engineering, University of Arkansas, Fayetteville, AR 72701, USA
[b] Department of Biomedical Engineering, University of Arkansas, Fayetteville, AR 72701, USA
[c] AstraZeneca, R&D, Gaithersburg, MD 20878, USA

ARTICLE INFO

Keywords:
AEX Membrane Chromatography
Protein Purification
Virus Binding
MVM

ABSTRACT

Mobile and stationary phase factors were investigated in order to identify conditions for effective capture of minute virus of mice (MVM), a potential adventitious contaminant in biomanufacturing, using anion exchange membrane chromatography (AEX). The initial study was conducted for Membrane A for a range of feed conditions using bovine serum albumin (BSA) as a model protein mimicking acidic host-cell proteins (HCPs) competitive for virus binding. The effects of pH (6–8), salt concentration (0–150 mM NaCl) and level of BSA (0–10 g/L) were systematically investigated. It was found that higher BSA concentration has the most negative impact on MVM binding followed by the increased conductivity of the feed solution. The effect of pH on MVM binding is also detected but has a less impact compared to other two factors in the range of feed conditions investigated. In addition to Membrane A, three other AEX membranes (Membrane B, C and D) were investigated for MVM binding at a selected feed condition. Based on properties of the membranes investigated, it was found that ligand charge density has the most significant impact on MVM binding performance of AEX membranes from stationary phase perspective.

1. Introduction

The purification of monoclonal antibodies (mAbs) and other protein-based therapeutics routinely begins with a capture chromatography step [1,2], followed by chromatographic polishing steps including anion exchange (AEX), cation exchange (CEX), or hydrophobic interaction chromatography (HIC) [3–5]. In agreement with ICH Q5A [6], at least two viral clearance steps with orthogonal mechanisms are recommended by the Drug and Food Administration (FDA) [7]. Virus clearance steps may include low pH or detergent virus inactivation, AEX chromatography for virus removal, and virus retentive filtration [4,8–11]. Manufacturers must demonstrate an adequate overall viral safety profile prior to obtaining regulatory approval for product licensure.

AEX chromatography typically binds negatively charged virus particles as well as impurities such as host cell proteins (HCPs) and host cell DNA. In mAb purification, AEX is typically run in a flowthrough mode at neutral pH because mAbs tend to have basic isoelectric points (pIs) and are positively charged. Virus spiking studies using parvovirus minute virus of mice (MVM) and retrovirus xenotropic murine leukemia virus (xMuLV) are commonly used, to model potential adventitious viruses as well as endogenous virus in Chinese hamster ovary cell culture, widely used in the production of recombinant proteins [1,11]. MVM is an adventitious virus that historically contaminated biomanufacturing processes [12].

The virus clearance capability of AEX media makes use of the fact that the apparent pIs of some viruses such as MVM and xMuLV are acidic at ~ 6.0 [3,4,9–11,13] and become negatively charged under neutral buffer conditions. Therefore, virus bind to the positively charged AEX ligands of quaternary and primary amines under those conditions. However, competitive binding of other negatively charged impurities (HCPs and DNA) to the positively charged ligands could occur [3,4]. Depending on the level of impurity in the feed solution, competitive binding can potentially lead to a reduction in viral clearance. As a result, virus clearance could be affected by the presence of impurities in feed streams.

* Corresponding author.
E-mail address: xqian@uark.edu (X. Qian).

https://doi.org/10.1016/j.jchromb.2022.123449
Received 12 February 2022; Received in revised form 27 August 2022; Accepted 30 August 2022
Available online 13 September 2022

Table 1
Properties of membranes investigated.

Membrane	Membrane A	Membrane B	Membrane C	Membrane D
Base Membrane Material	Polyethersulfone	Stabilized Reinforced Cellulose	Stabilized Reinforced Cellulose	Polyacrylamide Composite
Membrane Volume (mL)	0.86	0.08	1.0	0.2
Ligand Type	Quaternary Amine	Primary Amine	Quaternary Amine	Quaternary Amine

The charges on HCPs and virus particles as well as on protein therapeutics depend on solution pH and conductivity [14–16]. Conductivity of the feed solution affects electrostatic interaction significantly as high conductivity (or ionic strength) reduces electrostatic interaction due to the screening effect.

Primary and quaternary amines are common AEX ligands. The strength of electrostatic interaction depends strongly on the magnitude of the charges on the positively charged ligands and negatively charged impurities. As a weak base, the charge on the primary amine ($-NH_2$) is affected by its pK_b value and buffer pH. In addition, primary amine is both a donor and acceptor for hydrogen bonding interaction in addition to the electrostatic interaction. Quaternary amine ($-NR_4^+$ or Q) cannot form hydrogen bonds with other functional groups. The charge on the quaternary amine remains approximately the same for a broad range of solution pH and conductivity.

Binding capacity could be affected by the ligand type and the charge density of the ligand as well as other stationary properties such as pore size, porosity and pore-size distribution. In particular, the relative size of the solute to that of the pore affects the accessibility of the ligands to the solute molecules of different sizes. Due to the variation in geometry between different adsorptive membranes, there could have intrinsic differences in the partitioning of the solute particles between the mobile and stationary phases. Given this interplay between many variables, it is expected that robustness for virus binding can vary, between AEX membranes. There have been no study investigating systematically the robustness of both the mobile and stationary phase properties on virus clearance during AEX chromatography.

The purpose of this study was to understand the effects of mobile and stationary phases on the robustness of virus binding from four commercial AEX membranes A, B, C, and D. Different operating conditions typically encountered in purification processes were tested. MVM, a parvovirus was used as a model because variable degrees of parvovirus removal were observed in previous studies [9,17]. Robustness was hypothesized to be affected by two groups of variables: feed/mobile phase attributes (pH, salt concentration, and impurity level represented by BSA) and stationary phase attributes (ligand type, ligand density, pore size, porosity and possibly other membrane properties). Here virus removal performance was investigated varying the pH, ionic strength, and impurity concentration. Based on the observed data, a phenomenological model was developed to demonstrate the interaction behavior between the variable parameters and binding of the virus. During the first part of the study, bovine serum albumin (BSA, pI 5.4) was used as a model acidic HCP [18] to investigate the effect of HCP level on MVM binding using Membrane A. Membrane A was more broadly used by biopharmaceutical industry compared to other three membranes. One feed condition that exhibited the highest sensitivity to MVM binding for membrane A was selected for the investigation of three additional commercial AEX membranes B, C and D. The second part of the study focused on confirming the findings in antibody containing feed solutions with different levels of impurities from their actual manufacturing processes.

2. Experimental approaches

2.1. Design of chromatographic experiments

Design of Experiments (DOE) provides an effective way for selecting experimental conditions and generating prediction models [19,20]. The effects of feed conditions including pH (6, 7, 8), salt concentration (0, 50, 150 mM NaCl) and the level of competition in terms of the BSA concentration (0, 1, 10 g/L) on MVM binding in 50 mM tris buffer were investigated initially with AEX Membrane A. The feed streams were spiked with 7.5 logs/mL (copies by qPCR) MVM. A custom DOE to determine the impacts of pH, conductivity (as measured by the NaCl concentration) and BSA levels was performed for a total of 14 feed conditions. All runs were conducted in duplicate with a fixed flowrate of 2 mL/min.

Membrane A-D were tested using an AKTA FPLC (GE Healthcare, Piscataway, NJ) with Unicorn software version 5.3. Membranes were wetted, and equilibrated as described earlier [4]. The feed volumes in the range of 1–20 mL to reach the same BSA loading density per membrane volume (MV) were used. The flowthrough, washing and elution fractions were collected separately. Each membrane was first equilibrated in adsorption buffer (feed buffer) for 10 min before use. After loading, the membrane was then washed with the same volume of the adsorption buffer, followed by elution using the elution buffer (feed buffer with 1 M NaCl). Protein concentrations in different fractions were determined using UV absorbance at 280 nm based on a standard curve. MVM titers were determined by median tissue culture infective dose ($TCID_{50}$) assay. The log reduction value (LRV) of the virus particles was calculated using the following formula:

$$LRV = log \frac{C_{MVM,feed}}{C_{MVM,flow-through}} \quad (1)$$

where $\boldsymbol{C_{MVM,feed}}$ and $\boldsymbol{C_{MVM,flow-through}}$ are the MVM titers in the feed and flow-through fractions. It is important to point out that the LRV values reflect the binding strength of MVM in the context of flowthrough AEX.

2.2. Material and methods

Membranes Commercially available AEX membranes were purchased from manufactures. Table 1 shows the properties of the membranes including membrane materials, membrane volume of the scale-down models used and ligand type.

Reagents Tris and sodium chloride (biotechnology grade) were purchased from G-Biosciences (Saint Louis, MO). Sodium hydroxide (ACS grade, ≧98 %), hydrochloric acid (6 mol/L), and Spectra/Por® 1–5 Standard RC Dry Dialysis Trial Kits (Spectrum® Laboratories) were purchased from VWR (Radnor, PA). Sodium phosphate dibasic (ReagentPlus®, ≥99.0 %) and sodium phosphate monobasic monohydrate (ACS reagent, ≥98 %) were purchased from Sigma-Aldrich (St. Louis, MO). Bovine serum albumin (BSA) was purchased from Lee BioSolution (Maryland Heights, MO). DNase for quantitative PCR was purchased from Promega (Madison, WI). iTaq universal SYBR green supermix was purchased from Bio-Rad (Hercules, CA), QIAquick PCR purification kit was purchased from Qiagen (Germantown, MD), TOPO® TA Cloning® Kit for Sequencing was purchased from Life Technologies (Carlsbad, CA), and One Shot™ TOP10 Chemically Competent *E. coli* was purchased from Thermo Scientific (Waltham, MA).

Feed Streams Buffers containing 50 mM Tris and 0, 50 or 150 mM NaCl were prepared initially. The pH of the buffers was then adjusted by titrating 2 M HCl into the above prepared buffers to reach targeted value of 6, 7 and 8. Proteins in the feed streams include BSA and human IgG1

(mAb A and mAb B). mAb A, purified after Protein A capture chromatography and AEX polishing steps, and mAb B, purified after Protein A capture chromatography only, were provided by AstraZeneca (Gaithersburg, Maryland, U.S.). Both mAbs have a pI of ~ 8.0. The HCP concentration in the more purified mAb A was less than 100 ppm whereas in less purified mAb B was in the order of ~ 500 ppm. These concentrations were measured by the same assay based on a proprietary HCP ELISA method. An ultrafiltration/diafiltration (UF/DF) step was used to prepare the feed stream to 50 mM tris buffer at pH 7 with 50 mM NaCl. The targeted mAb concentration after UF/DF was 10 g/L. The mAb feed concentration as well as feed volume were used to adjust the membrane loading density investigated.

Charge Density Measurement Surface charge densities and volume-based charge densities were obtained from manufacturers for membranes B and C. The volume-based charge densities of membrane A and D were determined by titration method, as described below. Membranes were initially rinsed by deionized (DI) water for 30 min. These membranes were then soaked in 0.1 M NaOH solution overnight. After that, membrane samples were washed again by the DI water until the pH of the solution reached 7. Thereafter, membranes were immersed in 2 M NaCl overnight to exchange the OH^- ions with Cl^- ions (both being counter ions to the positively charged amine groups in the membranes). The solutions after the ion exchange were then titrated using 0.01 M HCl to determine the number of OH^- ions being exchanged. The charge density is defined as the number of OH^- ions per unit membrane volume [3]. The corresponding surface charge densities were derived from the volume charge densities except for Membrane D which has a 3-D matrix structure.

Membrane Porosity Determination To determine the porosity of membranes investigated, lysozyme was used as a tracer as described elsewhere [21]. Experiments were conducted using 50 mM Tris containing 250 mM NaCl at pH 8. Lysozyme was dissolved in the buffer to reach 2 g/L concentration. Membranes were initially equilibrated with the buffer solution without the protein for 30 min. A total of 10 mL of prepared lysozyme solution was then injected and effluent was monitored by UV absorbance at 280 nm. The injection experiment performed at 5 different flow rates in the presence and absence of membranes. Lysozyme retention volume was calculated based on the average value from experiments with five flow rates, all within the recommended operation range by manufacturers. The porosity is determined as the percentage of the pore volume to the membrane volume.

MVM Production and Purification Minute virus of mice (MVM) is a representative parvovirus that can infect Chinese Hamster Ovary (CHO) cell culture. The initial stock of the MVM (ATCC® VR1346™) was purchased from American Type Culture Collection (Manassas, VA). A further production and purification of MVM were performed based on an adapted protocol from literature [22]. In-house produced MVM stocks typically have a titer of ~ 10.5–11.5 logs/mL measured by qPCR. The overall HCP concentration in the virus stock was determined to be less than 0.4 g/L. During MVM spiking studies, the targeted virus titer is 7.5 logs/mL (qPCR) using less than 100 μ L of the virus stock for a 20–60 mL feed stream. As a result, the HCP concentration from the virus stock in the feed is low, on the order of 10^{-4}-10^{-5} g/L. More details on the production and purification of our in-house produced MVM virus stock is described in a previous publication [8].

2.3. MVM titration assays

Quantitative PCR (qPCR) qPCR method was used to quantify the number of copies of viral genomes in virus stock and feed stream by a Bio-Rad CFX Connect™ Real Time System (Hercules, CA) with Bio-Rad CFX Manager software. The standard curve was made by qPCR amplification of serial diluted recombinant plasmid ranging from 10^1-10^9 copies/mL. Three repeats were done to plot the standard curve, with 95 % confidence limit and a mean ± 0.5 log considered as an acceptable criterion. More details on the qPCR protocol can be found in an earlier publication [8].

Table 2
LRV for the AEX DOE Experiments with Membrane A.

Variables			Response	
pH	NaCl (mM)	BSA (g/L)	LRV (logs) ($TCID_{50}$)	LRV (logs) (LVP)
7	50	0	≥ 2.75 ± 0.17	≥ 4.71 ± 0.13
6	150	1	0.08 ± 0.23	N/A
6	0	0	≥ 2.42 ± 0.18	≥ 4.38 ± 0.18
8	50	10	0.09 ± 0.21	N/A
7	0	10	0.27 ± 0.22	N/A
8	0	1	≥ 3.08 ± 0.10	≥ 5.04 ± 0.08
7	0	0	≥ 3.17 ± 0.14	≥ 5.13 ± 0.11
7	0	1	2.25 ± 0.20	N/A
8	150	1	0.83 ± 0.25	N/A
6	50	1	1.59 ± 0.23	N/A
7	150	1	0.33 ± 0.25	N/A
8	150	0	1.75 ± 0.25	N/A
8	0	0	≥ 3.08 ± 0.13	≥ 5.04 ± 0.08
8	50	1	≥ 3.25 ± 0.17	5.07 ± 0.13
8	0	0	≥ 3.33 ± 0.10	≥ 5.04 ± 0.13

$TCID_{50}$ Assay Viral titer of the feed and the filtrate was determined by $TCID_{50}$ assay. Briefly, the indicator cell line NB324K was donated from Peter Tattersall at Yale University. The cells were seeded into 96-well plate to reach a desired confluency of 20–50 %. The samples were diluted in serial 10-fold dilutions with the seeding medium. Each dilution was inoculated onto one column (6-wells) at 100 µL/well. The negative control wells were inoculated with the same seeding medium. Plates were incubated in 5 % CO_2 incubator at 37 °C. After ten days, all the wells were inspected under microscope for cytopathic effect (CPE). Two replicates were done for each sample. Spearman-Kärber method [23] was used for calculation of $TCID_{50}$ titer. More details on the $TCID_{50}$ assay can be found in our previous publication [24].

Large Volume Plating (LVP) Assay LVP assay was also performed for the flowthrough samples when no CPE was observed with the $TCID_{50}$ assay. The indicator cells were cultured in a 96 well plate following the same procedure as for $TCID_{50}$ assay. The samples were diluted three times with the seeding medium by mixing 14 mL of seeding medium with 7 mL of the samples. Each diluted sample was transferred into 50 mL disposable polystyrene reservoir and mixed well. Finally, each sample was inoculated onto 96 wells at 200 µL/well. Plates were returned to 37 °C, 5 % CO_2 incubator. After ten days, all the wells were inspected under microscope for CPE effect. The virus titer was calculated based on the mode D from previous work [25] if virus-induced changes are observed in only a few wells of the LVP (less than15 % of all wells). If no virus - induced changes are observed for a sample, the virus titer is determined by the Poisson distribution at the 95 % confidence limits [26]. Standard error Se and the confidence limit C ($C = \pm 2\ S_e$) were calculated for each assay. More details on the LVP assay cab be found in our previous publication [24].

2.4. Statistical analysis

A phenomenological model using JMP software from SAS Institute (Cary, NC) was developed to understand the virus clearance (LRV) with regard to conductivity, pH and the HCP concentration (represented by BSA) in the feed.

3. Results and discussion

3.1. The effects of feed condition and BSA concentration on MVM clearance

The AEX chromatographic runs with Membrane A based on the custom DOE as shown in Table 2 were performed for a total of 14 feed conditions with 1 repeat. The LRVs on the fourth column were

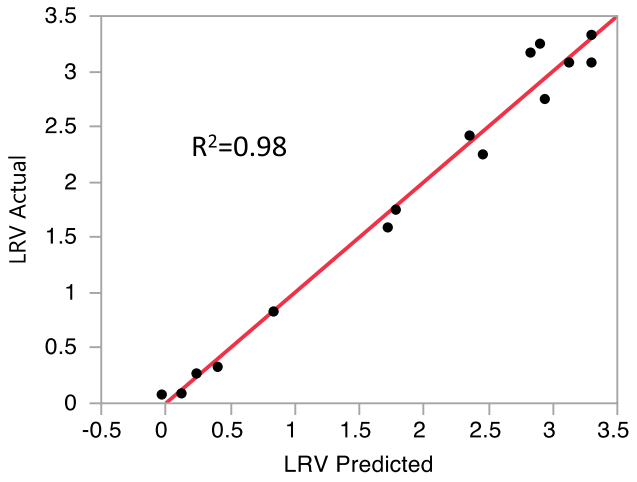

Fig. 1. The correlation between the predicted LRVs and $TCID_{50}$ infectivity assay measured LRVs for the DOE experiments with Membrane A.

Table 3
Significance of the regression coefficient in terms of P-values obtained from ANOVA analysis.

Variable Terms	P Ratio	Prob > P
pH	7.02	0.0381*
C_{NaCl} (mM)	10.9	0.0165*
C_{BSA} (g/L)	11.6	0.0143*
pH × C_{NaCl}	0.72	0.429
pH × C_{BSA}	2.98	0.135
C_{NaCl} × C_{BSA}	4.57	0.0765
C_{NaCl}^{2}	8.54	0.0266*

*P-value less than 0.05 indicates model terms are significant.

calculated based on the $TCID_{50}$ assay from both the feed and flow-through fractions. When no infective virus particle was detected in the flowthrough fraction, the assay detection limit was used in the calculation and the "≥" sign used to indicate that the LRV is larger or equal to the value calculated. Table 2 shows the feed conditions including pH, NaCl concentration in mM and BSA concentration in g/L, and the corresponding LRVs for MVM clearance. When no virus was detected with the $TCID_{50}$ assay, additional LVP assay was performed. These LRVs are then listed in the fifth column.

When the BSA concentration is 10 g/L or when the salt concentration is 150 mM, significant virus breakthrough was observed with LRV less than 1 except for one condition with a LRV of 1.75. BSA is a model HCP that binds competitively to prevent MVM binding as both are negatively charged in a solution above pH 6. A 10 g/L of BSA concentration could saturate the binding sites on the AEX membranes leading to a dramatic reduction in LRV to less than 0.5. On the other hand, the effect of 150 mM NaCl concentration without any BSA in the feed solution on virus binding is not as dramatic since the conductivity of the feed solution is still relatively low at ~ 19 mS/cm. Higher conductivity leads to a stronger charge screening effect and a weaker electrostatic interaction. When 150 mM NaCl is combined with some BSA (1 g/L), the impact on virus binding is more significant. In 6 of the 14 conditions, complete virus retention based on the assay detection limit was observed where conditions are favorable for MVM binding (low conductivity and low competition).

The LRVs from $TCID_{50}$ assay as a function of pH, NaCl and BSA concentrations using JMP do not fit well with a linear function. As a result, a second-order polynomial fit was carried out resulting an empirical equation (2) describing the relationship between LRV and the three independent variables:

$$LRV = -0.75 + 1.33 \times \Delta pH - 2.57 \times \%salt - 3.23 \times \%BSA - 0.12 \times \Delta pH \times \%salt + 0.98 \times \Delta pH \times \%BSA - 1.93 \times \%salt \times \%BSA - 0.61 \times (\%salt)^2 + 0.31 \times (\%BSA)^2 \quad (2)$$

where $\Delta pH = pH - 7; \%salt = \frac{C_{NaCl}-75}{75}; \%BSA = \frac{C_{BSA}-5}{5}$ *with* C_{NaCl} and C_{BSA} representing the concentrations of NaCl in mM and BSA in g/L in the feedstream respectively. Fig. 1 illustrates the correlation between predicted LRV and actual measurements with $TCID_{50}$ assay with $R^2 \sim 0.98$. Statistical ANOVA analysis shows that only the first-order salt and BSA concentration coefficients and the $(salt)^2$ coefficient are statistically significant with P values less than 0.05 as shown in Table 3. The first-order coefficients of the empirical relation (2) indicate that increasing pH enhances MVM binding, increasing BSA and NaCl concentrations has a stronger negative impact on MVM binding at the first order. One confirmation experiment was performed with the condition pH = 7, C_{NaCl} = 50 mM, C_{BSA} = 1 g/L. The predicted LRV is 2.33 logs close to the actual measured value of 2.75 logs. The second confirmation experiment was performed with the condition pH = 7, C_{NaCl} = 150 mM, C_{BSA} = 0.5 g/L. The predicted LRV is 0.97 logs in good agreement with the measured value of 1.00 logs.

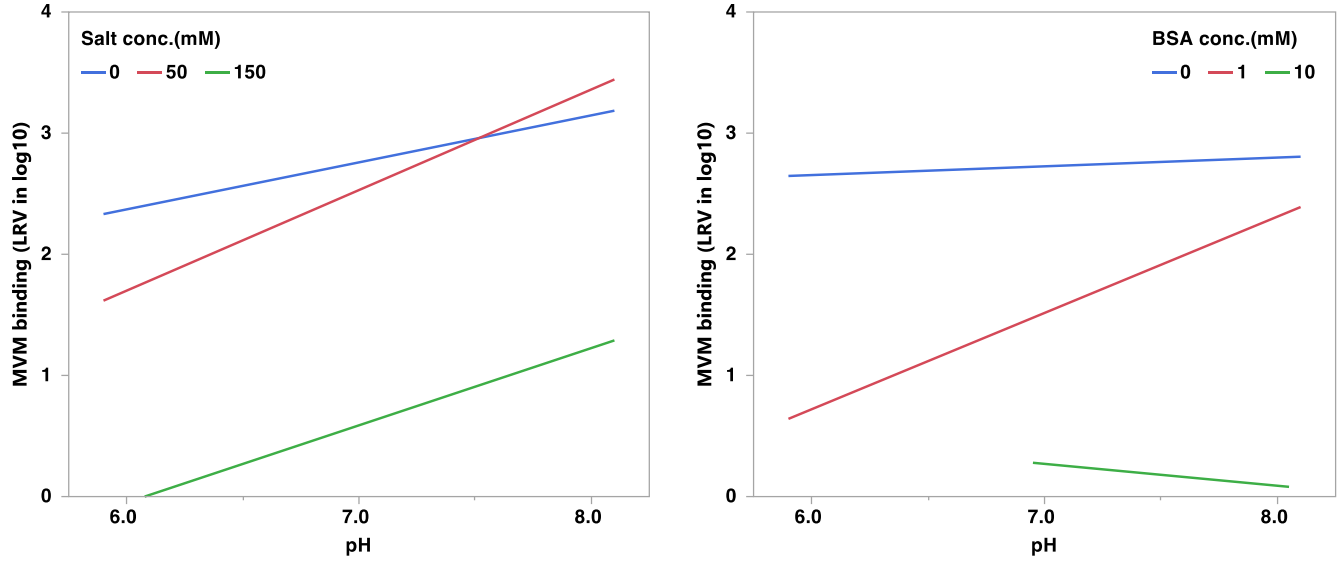

Fig. 2. The effects of pH on MVM binding at three different salt concentrations (left) and BSA concentrations (right) in the feed streams for Membrane A.

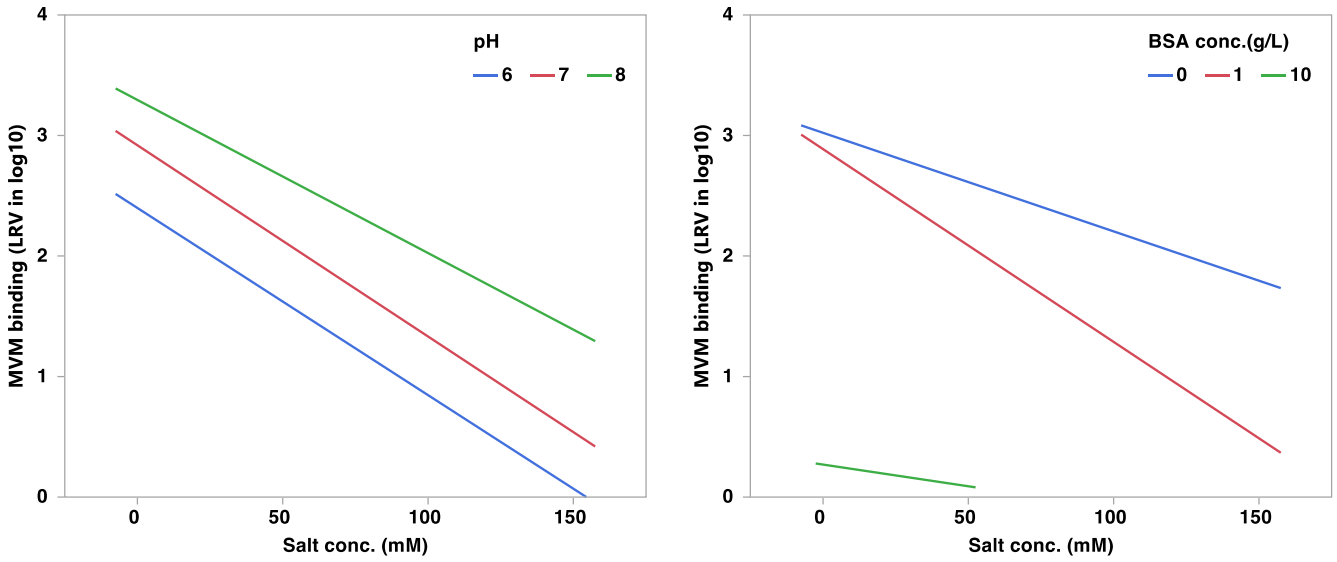

Fig. 3. The effects of salt concentration on MVM binding at three different pH values and levels of competition measured by BSA concentrations in the feed streams for Membrane A.

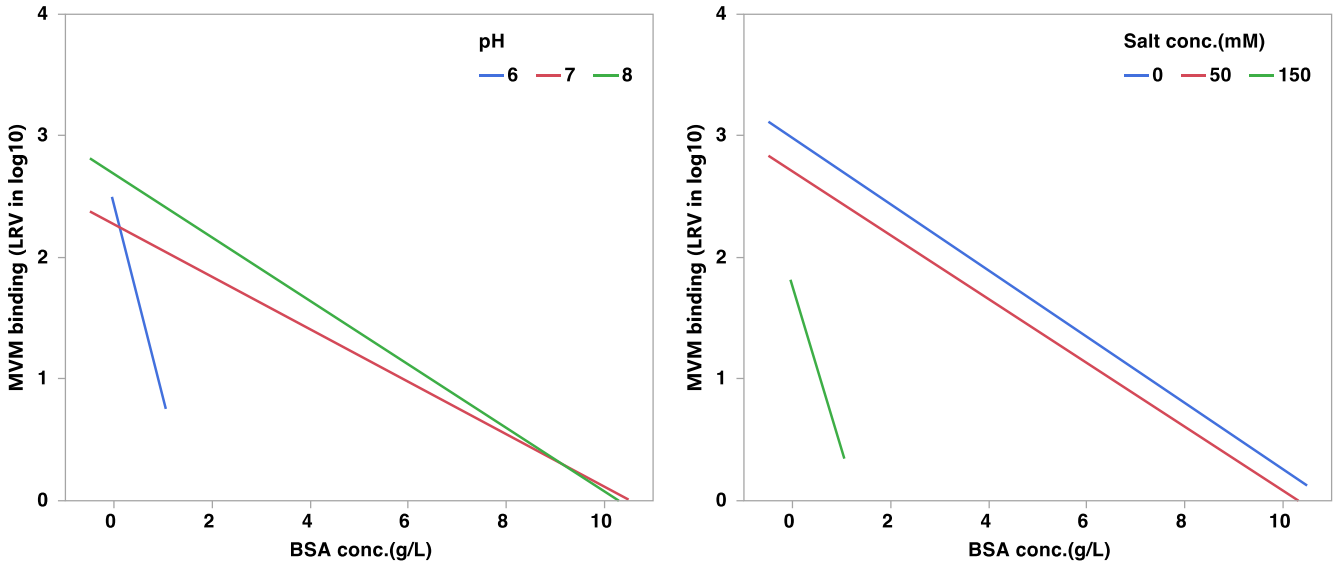

Fig. 4. The effects of level of competition measured by BSA concentrations on MVM binding at three different pH values and salt concentrations in the feed streams for Membrane A.

Fig. 2 plots the effects of pH on LRV for MVM binding at three different pH levels for three NaCl concentrations (left) and three BSA concentrations (right). LRV increases with the increase of pH for all three salt concentrations. This is due to the fact that the charge on MVM particle becomes more negative as the pH increases resulting in a stronger electrostatic interaction with the positively charged quaternary ammonium ion ligand which does not vary significantly with the change of pH. Fig. 2 also shows that the increase of LRV with pH is more sensitive to NaCl concentration at 50 mM compared to other two salt conditions. This is due to the fact that at higher salt concentration of 150 mM, the LRVs at all pH conditions are dominated by the weakened electrostatic interaction. At salt concentration of 50 mM, the increase in MVM charge with pH also contributes to the increase in LRV. The variation of LRV as a function of pH at three different BSA levels exhibits similar trend as shown on the right-hand panel of Fig. 2. The increase of BSA concentration in the feed dramatically reduced the LRV. At 10 g/L BSA, the LRV is reduced to almost zero. At 1 g/L BSA feed solution, LRV has the most apparent increases with the increase of pH. In the absence of BSA in the feed stream, no virus breakthrough was observed for all three pH conditions.

Fig. 3 shows the effect of salt concentration on MVM binding at three pH conditions (left panel) and at three BSA concentrations (right panel). It is apparent that the increase of salt concentration in the feed reduces MVM binding for all the conditions. It seems that solution conductivity has a stronger effect than the effect of pH change on MVM binding in the tested range. This can be inferred from equation (2) where the first-order coefficient for the salt concentration is higher than the corresponding value for pH and that second-order salt concentration term is also statistically significant, the only higher order term with P value less than 0.05.

Fig. 4 shows the effect of BSA concentration on MVM binding at different pH conditions (left-panel) and at three different salt concentrations (right-panel). It can be seen at both panels, the reduction in MVM binding is more dramatic as BSA concentration in the feed increases indicating that acidic HCPs in the feed can have a significant effect on virus binding. It can also be inferred from Equation (2) that the

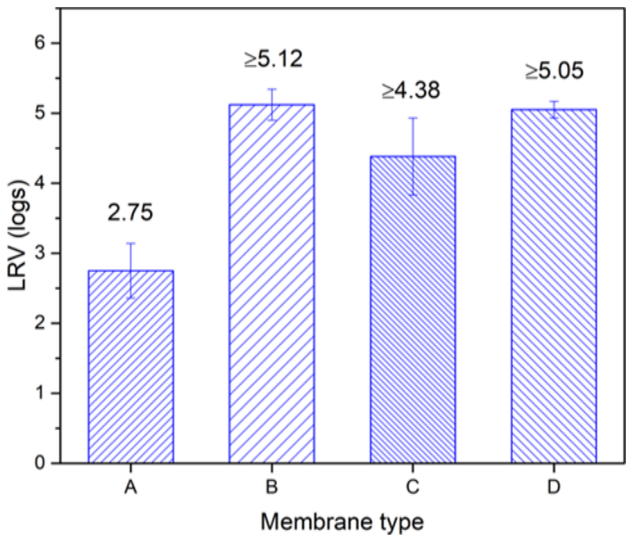

Fig. 5. Comparison of MVM binding measured by LRV for 4 commercially available anion exchange membranes under 50 mM Tris buffer at pH 7 with 50 mM NaCl. The feed contains 1 g/L BSA and ~ 7.5 logs (qPCR) MVM per mL of feed volume (equivalent to ~ 8.8 logs per mL of membrane volume).

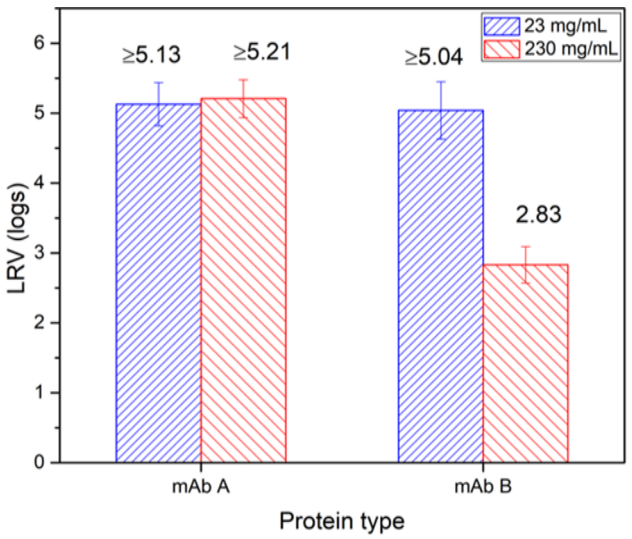

Fig. 6. LRV for MVM binding during AEX run with Membrane A for both mAb A and mAb B feed at two loading densities of 23 and 230 mg/mL MV in 50 mM Tris buffer at pH 7 with 50 mM NaCl.

Table 4
Membrane surface and volume charge densities, pore sizes and porosity for the four membranes investigated.

Membrane	Membrane A	Membrane B	Membrane C	Membrane D
Surface Charge Density (μeq/cm^2)	0.61	18–22	2–5	N/A
Volume Charge Density (mmol/mL)	0.056[a]	0.65–0.80[b]	0.072–0.18[b]	1.0[a]
Pore Size (μm)	0.8	3–5	3–5	0.4
Porosity (%)	64	–*	62	85

*Porosity not measured; [a]measured by this work; [b]obtained from the manufacturer.

first-order coefficient for BSA is the largest among the other two first-order coefficients. Therefore, during AEX virus binding, the HCP level in the feed may have the strongest effect, followed by the conductivity of the feed solution and finally the feed pH in the range of conditions investigated here. From above results for Membrane A, the binding variability is most noticeable when the condition at pH 7, 50 mM NaCl and 1 g/L BSA. This is also the condition at which the LRV remains high yet with observable virus breakthrough for Membrane A. As a result, this condition is used for the subsequent studies to investigate the effects of membrane type on MVM binding.

3.2. Comparison of AEX Membrane performance for MVM binding

Four anion exchange membranes (Membranes A, B, C, and D) were investigated side-by-side for MVM binding at the selected feed condition of pH 7 with 50 mM NaCl and 1 g/L BSA. Virus loading density was kept similar for all the membranes at ~ 8.8 logs (qPCR) MVM per mL of membrane volume (MV). The feed volume for each membrane was different depending on the individual membrane volume. It was ~ 20 mL for Membrane A (MV 0.86 mL) and Membrane C (MV 1.0 mL), 1 mL for Membrane B (MV 0.08 mL) and 2 mL for Membrane D (MV 0.2 mL). The $TCID_{50}$/LVP assay was used to determine the virus titers.

Fig. 5 shows the LRVs for the 4 different AEX membranes investigated. Since no virus breakthrough from $TCID_{50}$ assay was observed in the flowthrough fractions from the Membranes B, C, and D, the LRVs shown in Fig. 5 are from LVP assay in the flowthrough fractions from these three membranes. Virus breakthrough was detected for Membrane A resulting in a relatively low LRV. To better understand the performance differences in MVM binding between these AEX membranes, the pore structure and charge densities were compared. Table 4 lists surface and volume charge densities, pore sizes and porosities of these membranes. It can be seen that the pore size of Membrane A lies between those of Membrane D and Membrane C. The porosity of Membrane A is similar to that of Membrane C. These results indicate that pore size and porosity are not the major causes for the low LRV observed for Membrane A. However, the charge density of Membrane A is significantly lower than those of Membrane B, Membrane D and lower than that of Membrane C. This suggests that charge density could significantly impact the performance of MVM binding. This observation agrees with the previously proposed stoichiometric displacement (SD) model [27] and the later improved steric mass action model (SMA) [28]. Both models indicate that the binding capacity of an ion-exchange medium is directly correlated with the number of ligands or charges available on the medium. It is clear that charge density is more critical for MVM binding at the same virus loading challenge for the membranes investigated. This is particularly true for MVM binding since MVM particle sizes are in the range of 18–24 nm, much smaller than membrane pore sizes. For large virus particles, pore size and porosity may become more important.

3.3. MVM binding with mAb feed streams

MVM binding for mAb A and B were investigated using two AEX membranes, Membrane A and Membrane D with the lowest and highest charge density respectively. Both mAbs were buffer exchanged to the buffer matrix of 50 mM Tris at pH 7 with 50 mM NaCl as investigated previously. Two mAb concentrations were used at 1 g/mL and 10 g/mL to achieve different antibody loading densities of approximately 23–25 and 230–250 mg/mL MV respectively. In addition, a second set of experiments for Membrane D with mAb loading density of ~ 1000 mg/mL MV were also tested as this membrane demonstrated a much higher binding capacity compared to those of other membranes investigated.

Fig. 6 shows the LRV for MVM binding during AEX run with Membrane A for two mAbs at two different protein loading densities of 23 and 230 mg/mL MV. $TCID_{50}$ assay was used to determine the feed and flowthrough MVM titers. For more purified mAb A, the LRV reached over 5 at both loading densities. No virus breakthrough was observed in the

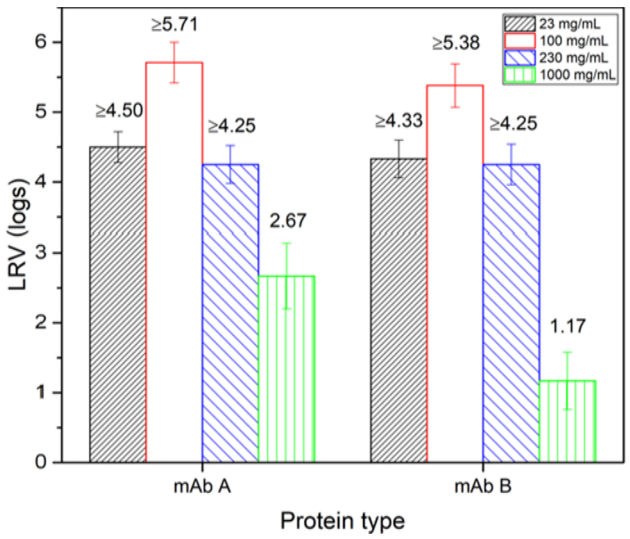

Fig. 7. LRV for MVM binding during AEX run with Membrane D for both mAb A and mAb B feed at loading densities of 25, 100, 250 and 1000 mg/mL MV in 50 mM Tris buffer at pH 7 with 50 mM NaCl. The higher LRV values observed at 100 mg/mL MV resulted from the initial higher virus titer in the feed.

flowthrough fractions. For less purified mAb B, the LRV also reached over 5 for the 23 mg/mL MV loading density indicating a high level of virus binding. However, at a loading density of 230 mg/mL MV, MVM breakthrough was observed and the LRV was reduced to 2.83 which confirms the finding that HCPs in the feed solution affect MVM binding to the AEX membrane, likely through competition for ligands.

Fig. 7 shows the LRV for MVM binding for Membrane D for both mAbs at four different loading densities of 25, 100, 250 and 1000 mg/mL MV in 50 mM Tris buffer at pH 7 with 50 mM NaCl. For all the runs except 1000 mg/mL loading density, LRV reached over 4 with no virus detected in the flowthrough. The higher LRVs observed at 100 mg/mL MV loading density resulted from the higher virus titer in the feed streams (8.5 logs/mL vs 7.5 logs/mL measured by qPCR). It indicates that Membrane D has a high MVM binding capacity, likely due to its high ligand density and/or unique structure. For both mAb A and mAb B, significant virus breakthrough was observed at 1000 mg/mL MV. For more purified mAb A, an LRV of 2.67 was obtained whereas for a less purified mAb B, an LRV of 1.17 was obtained again affirming the impact of HCP impurity on MVM binding.

4. Conclusions

Among the mobile phase factors, pH, conductivity and the concentration of BSA as a model HCP impurity, the effect of pH on MVM binding was important but has a less impact compared to the level of impurities and feed conductivity in the range of feed conditions investigated.

Of the stationary properties, pore size, porosity and charge density, for the four AEX membranes investigated for MVM binding at the selected feed condition, the charge density of the ligand (surface and volume) correlates positively with the MVM clearance of AEX membranes. Pore size and porosity of the membrane substrate do not appear to affect MVM binding. This indicates that MVM binding is dominated by the electrostatic interaction in agreement with the previous study and the stoichiometric displacement (SD) model as well as the revised steric mass action model (SMA). Finally, membrane A and membrane D with the lowest and highest charge densities respectively investigated for MVM binding with two mAb feedstreams with different concentrations of HCP confirms that impurity level impacts the binding of MVM. This result is consistent with the study using BSA as a model HCP. These findings are summarized in Fig. 8, which could be used to guide the optimization of virus removal in protein purification processes, and also in purification of virus vectors for gene therapy or vaccine purposes. The left column and schematic indicate low MVM binding condition whereas the right column and schematic show the high MVM binding condition. When optimizing MVM removal, a developer would first select a membrane with high surface charge density, but not limited by pore size and porosity. Next, the developer would select a loading pH above MVM pI of 6 but below the pI of product in a low salt buffer so that virus is captured and product is allowed to flow through the membrane. This step should be performed at the end of the purification train so that competition from acidic HCP with similar pI to MVM is minimum. These principles can be applied to capture virus vectors such as adeno-associated virus (AAV) and subsequently elute AAV in a high salt/acidic buffer.

CRediT authorship contribution statement

Shu-Ting Chen: Data curation, Formal analysis, Investigation, Software, Writing – original draft. **Wenbo Xu:** Data curation, Formal analysis. **Kang Cai:** Conceptualization, Investigation, Methodology, Project administration, Resources, Writing – review & editing. **Gisela Ferreira:** Funding acquisition, Resources, Writing – review & editing. **S. Ranil Wickramasinghe:** Conceptualization, Funding acquisition,

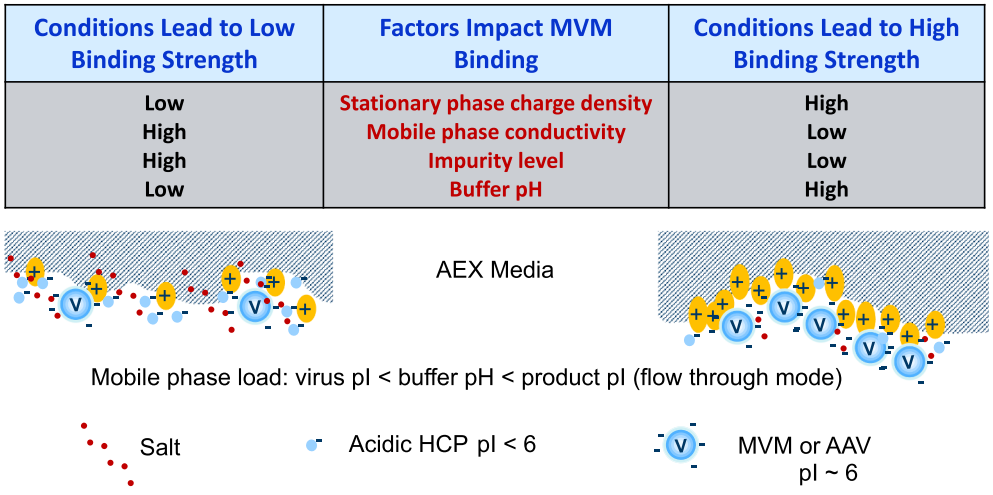

Fig. 8. Conditions promoting higher MVM binding strength: stationary phase with high surface charge density, mobile phase with low salt, low competitor, and virus carrying high net charge.

Methodology, Resources, Writing – review & editing. **Xianghong Qian:** Conceptualization, Formal analysis, Funding acquisition, Investigation, Methodology, Project administration, Supervision, Writing – original draft, Writing – review & editing.

Declaration of Competing Interest

The authors declare that they have no known competing financial interests or personal relationships that could have appeared to influence the work reported in this paper.

Data availability

Data will be made available on request.

Acknowledgement

Funding for this work was provided by AstraZeneca through the National Science Foundation Industry/University Cooperative Research Center for Membrane Science, Engineering and Technology, the National Science Foundation (IIP 1361809 and IIP 1822101) and the University of Arkansas. We also acknowledge MilliporeSigma for donating some of its membranes for the study. Assistance for some of the virus assay by Namila and Feng Xu is gratefully acknowledged.

References

[1] A.A. Shukla, J. Thömmes, Recent advances in large-scale production of monoclonal antibodies and related proteins, Trends Biotechnol. 28 (5) (2010) 253–261, https://doi.org/10.1016/j.tibtech.2010.02.001.
[2] B. Kelley, G. Blank, A. Lee, Downstream processing of monoclonal antibodies: current practices and future opportunities, Process Scale Purif. Antibodies (2009) 1–23.
[3] J. Weaver, S.M. Husson, L. Murphy, S.R. Wickramasinghe, Anion exchange membrane adsorbers for flow-through polishing steps: Part I. Clearance of minute virus of mice, Biotechnol. Bioeng. 110 (2) (2013) 491–499, https://doi.org/10.1002/bit.24724.
[4] J. Weaver, S.M. Husson, L. Murphy, S.R. Wickramasinghe, Anion exchange membrane adsorbers for flow-through polishing steps: Part II, Virus, host cell protein, DNA clearance, and antibody recovery, Biotechnology and bioengineering 110 (2) (2013) 500–510, https://doi.org/10.1002/bit.24720.
[5] C.H. Goey, S. Alhuthali, C. Kontoravdi, Host cell protein removal from biopharmaceutical preparations: Towards the implementation of quality by design, Biotechnol. Adv. 36 (4) (2018) 1223–1237, https://doi.org/10.1016/j.biotechadv.2018.03.021.
[6] ICH, VIRAL SAFETY EVALUATION OF BIOTECHNOLOGY PRODUCTS DERIVED FROM CELL LINES OF HUMAN OR ANIMAL ORIGIN Q5A(R1), 1999.
[7] FDA, FDA-Points to Consider in the Manufacture and Testing of Monoclonal Antibody Products for Human Use, in: U.S.D.o.H.a.H.S.F.a.D.A.C.f.B.E.a. Research (Ed.) 1997, p. 50.
[8] FNU Namila, D.a. Zhang, S. Traylor, T. Nguyen, N. Singh, R. Wickramasinghe, X. Qian, The effects of buffer condition on the fouling behavior of MVM virus filtration of an Fc-fusion protein, Biotechnol. Bioeng. 116 (10) (2019) 2621–2631, https://doi.org/10.1002/bit.27085.
[9] K. Cai, J. Anderson, J.D. Orchard, C.D. Afdahl, M. Dickson, Y. Li, Virus removal robustness of ion exchange chromatography, Biologicals 58 (2019) 28–34, https://doi.org/10.1016/j.biologicals.2019.01.004.
[10] G. Miesegaes, S. Lute, E. Read, K. Brorson, Viral clearance by flow-through mode ion exchange columns and membrane adsorbers, Biotechnol. Prog. 30 (1) (2014) 124–131, https://doi.org/10.1002/btpr.1832.
[11] D.M. Strauss, S. Lute, Z. Tebaykina, D.D. Frey, C. Ho, G.S. Blank, K. Brorson, Q. i. Chen, B. Yang, Understanding the mechanism of virus removal by Q sepharose fast flow chromatography during the purification of CHO-cell derived biotherapeutics, Biotechnol. Bioeng. 104 (2) (2009) 371–380, https://doi.org/10.1002/bit.22416.
[12] P.W. Barone, M.E. Wiebe, J.C. Leung, I.T.M. Hussein, F.J. Keumurian, J. Bouressa, A. Brussel, D. Chen, M. Chong, H. Dehghani, L. Gerentes, J. Gilbert, D. Gold, R. Kiss, T.R. Kreil, R. Labatut, Y. Li, J. Müllberg, L. Mallet, C. Menzel, M. Moody, S. Monpoeho, M. Murphy, M. Plavsic, N.J. Roth, D. Roush, M. Ruffing, R. Schicho, R. Snyder, D. Stark, C. Zhang, J. Wolfrum, A.J. Sinskey, S.L. Springs, Viral contamination in biologic manufacture and implications for emerging therapies, Nat. Biotechnol. 38 (5) (2020) 563–572, https://doi.org/10.1038/s41587-020-0507-2.
[13] T. Iskra, A. Sacramo, C. Gallo, R. Godavarti, S. Chen, S. Lute, K. Brorson, Development of a modular virus clearance package for anion exchange chromatography operated in weak partitioning mode, Biotechnol. Prog. 31 (3) (2015) 750–757, https://doi.org/10.1002/btpr.2080.
[14] H. Dong, H. Du, X. Qian, Theoretical prediction of p K a values for methacrylic acid oligomers using combined quantum mechanical and continuum solvation methods, The Journal of Physical Chemistry A 112 (49) (2008) 12687–12694, https://doi.org/10.1021/jp807315p.
[15] H. Dong, H. Du, X. Qian, Prediction of p K a Values for Oligo-methacrylic Acids Using Combined Classical and Quantum Approaches, J. Phys. Chem. B 113 (39) (2009) 12857–12859, https://doi.org/10.1021/jp9060889.
[16] H. Dong, H. Du, S.R. Wickramasinghe, X. Qian, The Effects of Chemical Substitution and Polymerization on the p K a Values of Sulfonic Acids, J. Phys. Chem. B 113 (43) (2009) 14094–14101, https://doi.org/10.1021/jp906087c.
[17] G. Miesegaes, M. Bailey, H. Willkommen, Q. Chen, D. Roush, J. Blümel, K. Brorson, Proceedings of the 2009 Viral Clearance Symposium, Developments in biologicals 133 (2010) 3-101.
[18] N. Aboulaich, W.K. Chung, J.H. Thompson, C. Larkin, D. Robbins, M. Zhu, A novel approach to monitor clearance of host cell proteins associated with monoclonal antibodies, Biotechnol. Prog. 30 (5) (2014) 1114–1124, https://doi.org/10.1002/btpr.1948.
[19] B. Qi, X. Chen, F. Shen, Y. Su, Y. Wan, Optimization of enzymatic hydrolysis of wheat straw pretreated by alkaline peroxide using response surface methodology, Ind. Eng. Chem. Res. 48 (15) (2009) 7346–7353, https://doi.org/10.1021/ie8016863.
[20] K. Cai, J.L.C. Miller, C.J. Stenland, K.J. Gilligan, R.C. Hartwell, J.C. Terry, R. B. Evans-Storms, R. Rubenstein, S.R. Petteway, D.C. Lee, Solvent-dependent precipitation of prion protein, Biochimica et Biophysica Acta (BBA) - Protein Structure and Molecular Enzymology 1597 (1) (2002) 28–35.
[21] C. Boi, A. Malavasi, R.G. Carbonell, G. Gilleskie, A direct comparison between membrane adsorber and packed column chromatography performance, J. Chromatogr. A 1612 (2020) 460629, https://doi.org/10.1016/j.chroma.2019.460629.
[22] D.R. Asher, A.B. Katz, N.Z. Khan, U. Mehta, Methods of producing high titer, high purity virus stocks and methods of use thereof, EMD Millipore Corp EUROPE (2011).
[23] R. Dougherty, R. Harris, Techniques in experimental virology, RJC Harris, Ed (1964) 169.
[24] R. Fan, F. Namila, D. Sasongko, S.R. Wickramasinghe, J. Mi, D. Kanani, X. Qian, The effects of flux on the clearance of minute virus of mice during constant flux virus filtratoin, Biotechnol. Bioeng. 118 (9) (2021) 3511–3521, https://doi.org/10.1002/bit.27778.
[25] M. Gavasane, A.U. Ali, A. Samagod, J. Kaundinya, G. Daftary, T. Preuss, H. Ruppach, N. Shaligram, B. Raghunath, S. Banerjee, Process Development and Spiking Studies for Virus Filtration of r-hFSH, (2013).
[26] E.M.E. Agency, Note for Guidance on Quality of Biotechnological Products: Viral Safety Evaluation of Biotechnology Products Derived from Cell Lines of Human or Animal Origin (CPMP/ICH/295/95), European Medicines Evaluation Agency London (1997).
[27] W. Kopaciewicz, M. Rounds, J. Fausnaugh, F. Regnier, Retention model for high-performance ion-exchange chromatography, J. Chromatogr. A 266 (1983) 3–21, https://doi.org/10.1016/S0021-9673(01)90875-1.
[28] C.A. Brooks, S.M. Cramer, Steric mass-action ion exchange: displacement profiles and induced salt gradients, AIChE J. 38 (12) (1992) 1969–1978, https://doi.org/10.1002/aic.690381212.